

# Selective imaging in second-harmonic-generation microscopy with anisotropic radiation

Shi-Wei Chu,<sup>a,\*</sup> Shih-Peng Tai,<sup>b</sup> Tzu-Ming Liu,<sup>b</sup> Chi-Kuang Sun,<sup>b</sup> and Chi-Hung Lin<sup>c</sup>

<sup>a</sup>Department of Physics, National Taiwan University, Taipei 10617, Taiwan

<sup>b</sup>Graduate Institute of Photonics and Optoelectronics and Department of Electrical Engineering, National Taiwan University, Taipei 10617, Taiwan

<sup>c</sup>Institute of Microbiology and Immunology, National Yang-Ming University, Taipei 11221, Taiwan

**Abstract.** As a novel modality of optical microscopy, second-harmonic generation (SHG) provides attractive features including intrinsic optical sectioning, noninvasiveness, high specificity, and high penetrability. For a biomedical application, the epicollection of backward propagating SHG is necessary. But due to phase-matching constraint, SHG from thick tissues is preferentially forward propagation. Myosin and collagen are two of the most abundant fibrous proteins in vertebrates, and both exhibit a strong second-harmonic response. We find that the radiation patterns of myosin-based muscle fibers and collagen fibrils are distinct due to coherence effects. Based on these asymmetric radiation patterns, we demonstrate selective imaging between intertwining muscle fibers and type I collagen fibrils with forward and backward SHG modalities, respectively. Thick muscle fibers dominate the forward signal, while collagen fibril distribution is preferentially resolved in the backward channel without strong interference from muscle. Moreover, we find that well-formed collagen fibrils are highlighted by forward SHG, while loosely arranged collagen matrix is outlined by backward signal. © 2009 Society of Photo-Optical Instrumentation Engineers. [DOI: 10.1117/1.3080722]

Keywords: microscopy; second-harmonic generation; biomedical optics; tissues; anisotropy; nonlinear optics.

Paper 08310LR received Sep. 3, 2008; revised manuscript received Nov. 5, 2008; accepted for publication Dec. 21, 2008; published online Feb. 24, 2009.

Since the first demonstration, multiphoton imaging has proven itself to be an invaluable tool in biomedical research. The nonlinear excitation scheme features deep optical imaging and 3-D resolution in unstained and unsectioned live biological tissues. Second-harmonic generation (SHG), as one of the nonlinear excitation families, provides not only deep imaging and 3-D capabilities, but also intrinsic contrast in certain tissue components with crystalline structures. For instance, in plant tissue, polysaccharides such as starch and cellulose are known to exhibit strong SHG responses.<sup>1,2</sup> In animal tissue, type I collagen and type II myosin, which are

two of the most abundant structural proteins, are both dominant second harmonophores and have been extensively discussed in recent literatures.<sup>3-5</sup> The glial fibrillary acidic protein in astroglial filaments and tubulin-based spindles in cellular mitosis processes are other examples of active SHG emitters.<sup>6,7</sup>

Since SHG seems to be limited to crystallized structural proteins, it provides exceptional specificity in molecular imaging applications, similar to fluorescence tagging. But unlike most fluorescence signals, which require extrinsic labeling, SHG provides intrinsic contrast and avoids complicated sample preparation. Moreover, SHG is a coherent process, so SHG from adjacent molecules will interfere with each other. Thus, local structure symmetry strongly affects the radiation direction and polarization dependency of SHG emission due to phase-matching condition. Such structure dependency offers additional molecular contrast. For example, collagen and myosin are both rodlike molecules but respectively exhibit a triple-helical and a double-helical structure with distinct inclination angles. The tiny angular difference in the molecular structural level results in dramatic difference in SHG polarization anisotropy from these proteins.<sup>5</sup> We recently demonstrated selective SHG imaging of collagen and myosin based on polarization manipulation techniques.<sup>8</sup> In this letter we report selective SHG imaging based on anisotropic radiation from these dominant vertebrate tissue constituents.

Our homebuilt laser-scanning SHG microscope with forward and backward detection schemes was described previously.<sup>9</sup> A Cr:forsterite laser operating at 1230 nm was used as the light source to provide high penetration into biological tissues. A long-working distance water immersion objective [LUMPLFLW/IR 60×/NA (numerical aperture) 0.9, Olympus, Japan] was used to provide thick tissue imaging capability. The 615-nm SHG signal was extracted by a dichroic beamsplitter and an interference filter in both collection routes. There was no confocal pinhole in the scanning system to improve the backward collection efficiency. To correlate the forward and backward signal intensity, the same detectors were used in both collection routes. The forward- and backward-detection efficiencies were calibrated with multiphoton excited fluorescence, which exhibits an isotropic emission profile, from DNA-bounded Hoechst dye in hepatic cells.<sup>10</sup> Spectral measurements were obtained with a monochromator combined with a cooled charge-coupled device at the backward side port of the microscope. The interference filters were removed during spectral acquisition. The tissues for experiment were longitudinal sections of the Vastus lateralis muscle, which were dissected from the hind thigh of a laboratory mouse. The tissues were dissected and immersed in 10% nature buffer formalin for 48 h. The thick slices were hand-cut with approximately 200 to 300 μm thickness. The thin slices were prepared from paraffin-embedded tissue with 4 μm thickness at 20-μm intervals for serial section (Leica, RM2135).

With a 4-μm microtomic slice, the simultaneously acquired forward SHG (FSHG) and backward SHG (BSHG) images are shown in Figs. 1(a) and 1(b), respectively. A significant difference is found between the images, demonstrating the potential of selective imaging. The sarcomeres in the

\*Address all correspondence to Shi-Wei Chu, Department of Physics, National Taiwan University, 1 Roosevelt Rd., Sec. 4, Taipei 10617, ROC. Tel: +886-233665131; Fax: +886-223639984; E-mail: swchu@phys.ntu.edu.tw

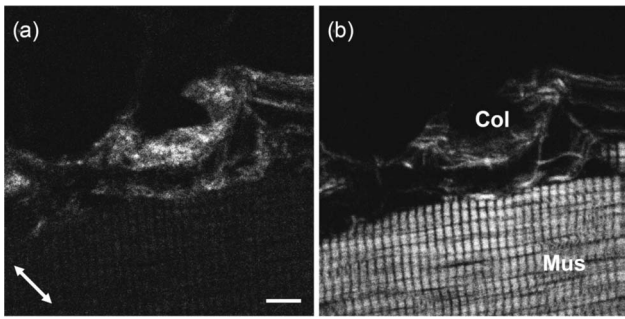


**Fig. 1** (a) BSHG and (b) FSHG images of a 4- $\mu\text{m}$  sliced muscular tissue with muscle fibers and adjacent collagen matrix clearly observable: arrow, laser polarization; Mus, muscle; Col, collagen; scale bar, 10  $\mu\text{m}$ .

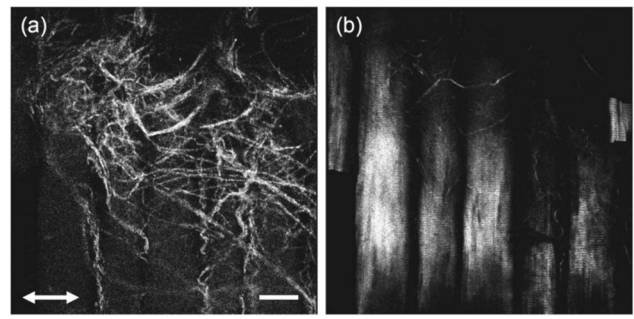


**Fig. 3** Selective imaging in a thick muscle tissue: (a) BSHG showing detailed collagen fibril distribution and (b) FSHG dominated by muscle fibers. Arrow, laser polarization; scale bar, 30  $\mu\text{m}$ .

skeletal muscle fibers and the type I collagen fibrils around the muscle are both observed in the FSHG image, while in the BSHG image, only collagen fibrils can be clearly identified. Here the image contrast is defined as  $\text{contrast} = (\text{SHG}_{\text{collagen}} - \text{SHG}_{\text{muscle}}) / \text{SHG}_{\text{muscle}}$  in the muscle-collagen complex. For thin-sliced samples sandwiched between a cover glass and a slide glass, the contrast in FSHG is  $-0.74 \pm 0.03$  and in BSHG is  $7.9 \pm 0.7$  (averaged over 10 samples).

To examine the second-harmonic nature of signals in the backward collection route, spectral analysis and power dependency are performed in both collagen/muscle tissue types, as shown in Fig. 2. From Fig. 2(a), symmetric SHG peaks centered at 615 nm are observed in both tissues, while weak two-photon-excited autofluorescence around 650 nm is observed only in collagen, in agreement with a recent report.<sup>11</sup> Since 615-nm interference filters with 10-nm bandwidth were inserted right before the detectors and the SHG at 615 nm is significantly stronger than the autofluorescence, it is reasonable to state that the scanned images are comprised of SHG signals only, without fluorescence contamination. The SHG nature of the backward emission from collagen and muscle fibers is further confirmed by the quadratic power dependency in Fig. 2(b).

In Fig. 3, we demonstrate large-scale selective SHG imaging in the thick muscle tissue. FSHG is dominated by strong signals from muscle fibers, while detailed collagen fibril distribution is revealed through BSHG modality. Very few collagen fibrils are still visible in the forward direction. Due to the extraordinarily strong SHG from muscle fibers, the detector gain must be lowered to prevent saturation during FSHG

acquisition. This further suppresses the visibility of collagen fibrils in the forward direction, resulting in poor FSHG contrast as  $-0.76 \pm 0.07$ . On the other hand, the contrast in BSHG is enhanced to be  $9.34 \pm 1.0$ . These numbers agree well with previous literature<sup>12</sup> considering the maximal FSHG intensity from muscle fibers is about three times of that from collagen fibrils in our case. From the contrast comparison, it is evident that muscle fibers are suitable to be observed with the FSHG modality while collagen fibrils should be monitored with BSHG to avoid strong interference from muscle.

It is vital to determine the origin of BSHG from these structural proteins. We have shown that the FSHG/BSHG ratio in muscle fibers is significantly larger than that in collagen fibrils, similar to a recent report.<sup>12</sup> As a coherent process, SHG is predominantly forward-directed in common SHG-active materials due to phase-matching requirement, which is the case in muscle fibers. The origin of BSHG from a muscle fiber is back reflection of FSHG at muscle/glass interface in the thin slice sample, and is dominated by backscattering of FSHG in the thick one. In thick tissues, BSHG is less than 1% of the forward signal power.<sup>12</sup> With this diminishing BSHG, the detail of muscle fibers is best resolved in the forward direction. But when the interaction length is less than  $\lambda_{2\omega} / 2\pi \approx 100$  nm, phase matching is relaxed and both FSHG and BSHG will be generated.<sup>13</sup> For dispersive type I collagen matrix around muscle fibers, the fibril thickness is of the order of 100 nm, and thus BSHG is mainly contributed to by direct backward generation with comparable FSHG. Note that a few thicker collagen fibrils are still perceptible in FSHG, as shown in Fig. 3(b).

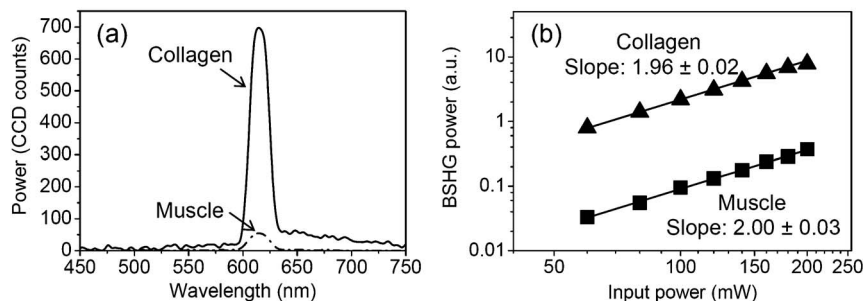


**Fig. 2** (a) Spectra and (b) power dependency in the backward collection route.

The correlation between FSHG/BSHG power ratio and fibril thickness has been found in collagen<sup>14</sup> and astroglial filaments,<sup>6</sup> and has been applied to estimate the thickness of individual collagen fibril.<sup>9</sup> Similar size dependence of forward versus backward signal has been observed with coherent anti-Stokes Raman scattering (CARS) microscopy,<sup>15</sup> though CARS is a  $\chi^{(3)}$  process, while SHG is a  $\chi^{(2)}$  process. The different backward and forward intensity profiles highlight the difference of coherent microscopy from incoherent microscopy and provide the basis for selective SHG imaging between muscular and collagen tissues.

Another noteworthy point is that BSHG from collagen seems not to colocalize well with FSHG from collagen in the scanned images. For instance, the profiles of collagen tissue in Fig. 1 are similar in both forward and backward directions, but the FSHG image reflects more fibrillar structures, while BSHG provides overall collagen distribution. This intriguing difference reveals more information regarding collagen distribution and may be explained in terms of coherent interaction in the forward and backward directions. The coherence length of SHG in collagen is about 100 nm in the backward direction but is about 10  $\mu\text{m}$  in the forward direction, much larger than collagen fibril diameters. SHG intensity is expected to be proportional to the square of active harmonophore numbers within single coherence length, so the contrast of well-formed thick collagen fibers is prominent in FSHG. But for BSHG with small coherence length, both well-formed fibers and loosely arranged collagen matrix exhibit similar signal intensity, resulting in somewhat more uniform signal distribution.

In conclusion, we demonstrated selective imaging of collagen and muscle tissues with the BSHG and FSHG modalities, respectively. Strongly enhanced contrast of collagen over muscle is observed in both microtomic and thick tissue samples in the backward collection route. In muscle fibers, BSHG is dominated by back reflection in a thin slice and diminishing backscattering in a thick sample, respectively. Thus, muscle fiber distribution is better resolved with FSHG imaging modality. On the other hand, collagen fibrils exhibit strong BSHG from direct backward generation and are appropriate for selective observation in the backward direction. Besides direct mapping of SHG signals, the ratio analysis of FSHG/BSHG may provide a more sensitive probe to local fibril thickness variation. The thick tissue imaging and optical sectioning capability make BSHG an eligible modality for clinical application, but the applicability may be limited to certain structural proteins due to the anisotropic radiation pattern.

## Acknowledgment

All tissue slices were kindly provided by Yung-Chih Chen and Bai-Ling Lin from the Development Center for Biotechnology, Taipei, Taiwan. This work was supported by National Science Council (Contracts No. NSC-95-2112-M-002-056-MY3 and No. NSC-96-2622-M-002-001-CC3) and National Taiwan University (97R0323).

## References

1. O. Nadiamykh, R. LaComb, P. J. Campagnola, and W. A. Mohler, "Coherent and incoherent SHG in fibrillar cellulose matrices," *Opt. Express* **15**(6), 3348–3360 (2007).
2. G. Cox, N. Moreno, and J. Feijo, "Second-harmonic imaging of plant polysaccharides," *J. Biomed. Opt.* **10**(2), 024013 (2005).
3. C. Odin, Y. Le Grand, A. Renault, L. Gailhouse, and G. Baffet, "Orientation fields of nonlinear biological fibrils by second harmonic generation microscopy," *J. Microsc.* **229**(1), 32–38 (2008).
4. A. Erikson, J. Ortegren, T. Hompland, C. D. Davies, and M. Lindgren, "Quantification of the second-order nonlinear susceptibility of collagen I using a laser scanning microscope," *J. Biomed. Opt.* **12**(4), 044402 (2007).
5. F. Tiaho, G. Recher, and D. Rouede, "Estimation of helical angles of myosin and collagen by second harmonic generation imaging microscopy," *Opt. Express* **15**(19), 12286–12295 (2007).
6. Y. Fu, H. F. Wang, R. Y. Shi, and J. X. Cheng, "Second harmonic and sum frequency generation imaging of fibrous astroglial filaments in ex vivo spinal tissues," *Biophys. J.* **92**(9), 3251–3259 (2007).
7. S. W. Chu, S. Y. Chen, T. H. Tsai, T. M. Liu, C. Y. Lin, H. J. Tsai, and C. K. Sun, "In vivo developmental biology study using noninvasive multi-harmonic generation microscopy," *Opt. Express* **11**(23), 3093–3099 (2003).
8. S. W. Chu, S. P. Tai, C. K. Sun and C. H. Lin, "Selective imaging in second-harmonic-generation microscopy by polarization manipulation," *Appl. Phys. Lett.* **91**(10), 103903 (2007).
9. S. W. Chu, S. P. Tai, M. C. Chan, C. K. Sun, I. C. Hsiao, C. H. Lin, Y. C. Chen, and B. L. Lin, "Thickness dependence of optical second harmonic generation in collagen fibrils," *Opt. Express* **15**(19), 12005–12010 (2007).
10. S. W. Chu, S. P. Tai, C. L. Ho, C. H. Lin, and C. K. Sun, "High-resolution simultaneous three-photon fluorescence and third-harmonic-generation microscopy," *Microsc. Res. Tech.* **66**(4), 193–197 (2005).
11. F. J. Kao, "The use of optical parametric oscillator for harmonic generation and two-photon UV fluorescence microscopy," *Microsc. Res. Tech.* **63**(3), 175–181 (2004).
12. F. Legare, C. Pfeffer, and B. R. Olsen, "The role of backscattering in SHG tissue imaging," *Biophys. J.* **93**(4), 1312–1320 (2007).
13. J. Mertz and L. Moreaux, "Second-harmonic generation by focused excitation of inhomogeneously distributed scatterers," *Opt. Commun.* **196**(1–6), 325–330 (2001).
14. R. M. Williams, W. R. Zipfel, and W. W. Webb, "Interpreting second-harmonic generation images of collagen I fibrils," *Biophys. J.* **88**(2), 1377–1386 (2005).
15. J. X. Cheng, A. Volkmer, and X. S. Xie, "Theoretical and experimental characterization of coherent anti-Stokes Raman scattering microscopy," *J. Opt. Soc. Am. B* **19**(6), 1363–1375 (2002).